

Zinc-oxide/PDMS-clad tapered fiber saturable absorber for passively mode-locked erbium-doped fiber laser

F D Muhammad, S A S Husin, E K Ng, K Y Lau, C A C Abdullah, M A Mahdi

Citation: Chin. Phys. B, 2021, 30 (**5**): 054204. DOI: 10.1088/1674-1056/abd76e
Journal homepage: http://cpb.iphy.ac.cn; http://iopscience.iop.org/cpb

What follows is a list of articles you may be interested in

Pulse generation in Yb-doped polarization-maintaining fiber laser by nonlinear polarization evolution

Cheng-Bin Liang(梁成斌), Yan-Rong Song(宋晏蓉), Zi-Kai Dong(董自凯), Yun-Feng Wu(吴云峰), Jin-Rong Tian(田金荣), Run-Qin Xu(徐润亲)
Chin. Phys. B, 2020, 29 (**7**): 074206. DOI: 10.1088/1674-1056/ab8ac6

575-fs passively mode-locked Yb:CaF_2 ceramic laser

Cong Wang(王聪), Qian-Qian Hao(郝倩倩), Wei-Wei Li(李威威), Hai-Jun Huang(黄海军), Shao-Zhao Wang(王绍钊), Da-Peng Jiang(姜大朋), Jie Liu(刘杰), Bing-Chu Mei(梅炳初), Liang-Bi Su(苏良碧)
Chin. Phys. B, 2020, 29 (**7**): 074205. DOI: 10.1088/1674-1056/ab8ac5

Influences of annealing temperature on properties of Fe^{2+}: ZnSe thin films deposited by electron beam evaporation and their applications to *Q*-switched fiber laser

Du-Xin Qing(卿杜鑫), Shu-Tong Wang(王树同), Shou-Gui Ning(宁守贵), Wei Zhang(张伟), Xiao-Xu Chen(陈晓旭), Hong Zhang(张弘), Guo-Ying Feng(冯国英), Shou-Huan Zhou(周寿桓)
Chin. Phys. B, 2020, 29 (**5**): 054208. DOI: 10.1088/1674-1056/ab81f2

High gain fiber-solid hybrid double-passing end-pumped Nd: YVO_4 picosecond amplifier with high beam quality

Xueyan Dong(董雪岩), Pingxue Li(李平雪), Shun Li(李舜), Dongsheng Wang(王东生)
Chin. Phys. B, 2020, 29 (**5**): 054207. DOI: 10.1088/1674-1056/ab8218

Zinc-oxide nanoparticle-based saturable absorber deposited by simple evaporation technique for Q-switched fiber laser

Syarifah Aloyah Syed Husin, Farah Diana Muhammad, Che Azurahanim Che Abdullah, Siti Huzaimah Ribut, Mohd Zamani Zulkifli, Mohd Adzir Mahdi
Chin. Phys. B, 2019, 28 (**8**): 084207. DOI: 10.1088/1674-1056/28/8/084207

Zinc-oxide/PDMS-clad tapered fiber saturable absorber for passively mode-locked erbium-doped fiber laser*

F D Muhammad[1,†], S A S Husin[1], E K Ng[2], K Y Lau[3], C A C Abdullah[1], and M A Mahdi[2]

[1] *Department of Physics, Faculty of Science, Universiti Putra Malaysia, 43400 UPM Serdang, Selangor, Malaysia*
[2] *Wireless and Photonics Networks Research Centre, Faculty of Engineering, Universiti Putra Malaysia, 43400 UPM Serdang, Selangor, Malaysia*
[3] *Department of Electronics and Nanoengineering, Tietotie 3, Aalto University, 02150 Espoo, Finland*

(Received 1 December 2020; revised manuscript received 1 December 2020; accepted manuscript online 30 December 2020)

We propose and demonstrate a passively mode-locked erbium-doped fiber laser (EDFL) based on zinc-oxide/polydimethylsiloxane (ZnO/PDMS) saturable absorber (SA) that evanescently interacts with the light on a tapered fiber. The ZnO/PDMS composite is coated on the whole surface of the tapered fiber to guarantee the maximum efficiency of the SA device, with a measured insertion loss of 0.87 dB and a modulation depth of 6.4%. The proposed laser can generate soliton mode-locking operation at a threshold power of 33.07 mW. The generated output pulse yields a repetition rate and pulse width of 9.77 MHz and 1.03 ps, respectively. These results indicate that the proposed ZnO/PDMS-clad tapered fiber could be useful as an efficient, compatible, and low-cost SA device for ultrafast laser applications.

Keywords: zinc-oxide, saturable absorber, tapered fiber, mode-locked, fiber laser

PACS: 42.55.Wd, 42.60.Fc **DOI:** 10.1088/1674-1056/abd76e

1. Introduction

Mode-locked fiber lasers are of great interest to researchers due to their ability to generate ultrashort pulses, which can find potential applications in various fields, including spectroscopy, basic scientific research, material processing, metrology, telecommunications, and biomedical research.[1–6] Although mode-locking can be undertaken using active components, the passive scheme, such as using saturable absorbers (SAs), is preferable since additional switching electronics that lead to the bulkiness of the system are not required. In contrast to the active method, passively mode-locked by SAs provide a significant advantage of low complexity and ease of operation due to their simple design, which allows for the development of compact and cost-effective pulsed laser sources.

Various SAs have been implemented for passively mode-locked fiber laser generation, such as semiconductor saturable absorber mirrors (SESAMs),[7,8] carbon nanotubes,[9,10] graphene,[11–13] topological insulators (TIs),[14] and transition metal dichalcogenides (TMDs).[15] Apart from the aforementioned SAs, a significant amount of research has also been devoted to the development of a cheaper material as the SA with less complex fabrication for passive mode-locking. Recently, zinc-oxide (ZnO) has emerged as a strong candidate to be employed as the saturable absorber due to its superior properties such as large carrier density excitation,[16,17] high third-nonlinear coefficient,[16,18–20] and ultrafast recovery time,[16,17] making it highly attractive for optical applications.

In previous works, most of the ZnO-based SAs are integrated into the fiber laser cavity by sandwiching the ZnO thin film between two fiber ferrules.[16,19–21] Although this technique is simple and compatible, the sandwiched SA material is in physical contact with the fiber ends and is prone to thermal damage due to the direct interaction with light, which can reduce the lifetime of the SA and hinder the operation in the high-power regime. In addition, this technique also involves a small functionalized area of the SA, confined by the small area of the fiber core. This would inherently limit the nonlinear interaction length of the SA, which eventually degrades the pulse laser operation.

As an improved technique, the evanescent field interaction scheme has been exploited to overcome the aforementioned drawbacks of the sandwiched-based SAs. This scheme allows the SA to interact with the leaking interface wave that propagates in the microfiber structure, such as D-shaped fibers,[22–24] hollow-core fibers and tapered fibers.[25,26] In contrast to direct penetration of light into the SA material at the fiber ends, it has many advantages such as high power tolerance of the optical power-induced thermal damage, and longer lateral interaction length between SA material and the evanescent field of the propagating wave along the microfiber. To enhance the efficiency of the light-SA interaction in this scheme, it is imperative to have a nonblocking configuration of the SA device structure.[27] Among evanescent field interaction schemes, the SA-coated tapered fiber seems to be the most versatile method compared to other types of microfibers[28] since the fiber surface are maximally

*Project supported by the Ministry of Higher Education of Malaysia (MOHE) (Grant No. FRGS/1/2019/STG02/UPM/02/4).
†Corresponding author. E-mail: farahdiana@upm.edu.my
© 2021 Chinese Physical Society and IOP Publishing Ltd

utilized, thus allowing for maximum efficiency of the light–SA interaction. Several methods have been demonstrated for fabricating the SA-coated tapered-fiber, such as optical deposition,[29,30] direct spray-coating,[31] and pulse laser deposition (PLD).[32,33] However, direct deposition of SA material on the taper's surface introduces large scattering loss and exposes the device directly to the environment.[28] In addition, those aforementioned methods could not guarantee the all-surface deposition on the tapered fiber. Therefore, researchers have come up with the idea of coating the SA-polymer composite on the tapered fiber using an appropriate polymer with low refractive index,[27,28,34–36] which enables the SA to be well dispersed in the polymer topology, thus reducing the clustering effect as well as the scattering loss.[28] In addition, the polymer composite could protect the device from direct exposure to the environment and impurities to improve durability.[28]

In this paper, we demonstrate the fabrication of ZnO/PDMS polymer-composite wrapped around the whole surface of the tapered fiber to guarantee the maximum efficiency of the nonlinear effect of the ZnO with careful optimization of the coating process. This is achieved by embedding a tapered fiber in ZnO/PDMS polymer-composite solution and subsequently spreading the solution evenly throughout the tapered region to maximize the coating area. The ZnO/PDMS-clad tapered fiber is then employed as an SA to realize mode-locked pulse operation in an EDFL based on the evanescent field interaction scheme. The measured modulation depth of the SA is 6.4%, with an insertion loss of 0.87 dB. The proposed laser can generate soliton mode-locking operation at a threshold power of 33.07 mW. The generated output pulse yields a repetition rate and pulse width of 9.77 MHz and 1.03 ps, respectively. These results indicate that the proposed ZnO/PDMS-clad tapered fiber could be useful as a simple and low-cost SA device for ultrafast laser applications. To the best of the authors' knowledge, this is the first demonstration of mode-locked fiber laser achieved by using ZnO/PDMS-clad tapered fiber.

2. Device fabrication

ZnO used in this work is originally in the form of nanopowder with a nanoparticle size of $\sim$ 55 nm, which is synthesized by the sol-gel method. The synthesis process of the ZnO nanopowder has been described in detail in Ref. [37]. The ZnO nanopowder is firstly mixed with chloroform, $CHCl_3$ as the effective solvent for ZnO, with a concentration of 0.3 mg/ml, which can evaporate easily and dissolve in most types of polymers. The ZnO/$CHCl_3$ mixture is subsequently placed into a commercial ultrasonicator at 15 kHz and 10 W for 30 minutes to form a well-dispersed ZnO nanoparticle in $CHCl_3$ solution and to reduce particle agglomeration.

The procedure is continued with the fabrication of the ZnO/$CHCl_3$/polydimethylsiloxane (ZnO/$CHCl_3$/PDMS) mixture by mixing 10 ml of the prepared ZnO/$CHCl_3$ solution with 20 ml PDMS polymer. It must be noted that appropriate mixing and concentration of ZnO nanoparticles in the polymer is significant to reduce the excessive scattering losses. The ZnO/$CHCl_3$/PDMS mixture is stirred by using a magnetic stirrer and heated continuously at 80 °C until the mixture is reduced to approximately 10 ml, which takes about 7 hours to be completed. This thermal treatment is crucial towards ensuring the evaporation of $CHCl_3$, which needs to be removed to form the ZnO/PDMS polymer-composite mixture, as well as to increase the homogeneity and transparency of the final ZnO/PDMS composite. The PDMS is chosen as the host polymer in this work due to its high transparency and low refractive index of $\sim$ 1.40, which is lower than the refractive index of glass silica of the optical fiber core. In addition, the PDMS polymer can help to reduce the scattering effect, which would consequently reduce the transmission loss of the signal propagating in the tapered region.

Once the ZnO/PDMS polymer-composite mixture is ready, we fabricate the tapered fiber, which is drawn from a standard single-mode optical fiber via the heating and pulling technique using a GPX-3000 Vytran instrument. This technique works in a way that the fiber is stretched out by the heat produced from the flame to reduce the fiber diameter at the transition region. In this work, the fiber is tapered down to a waist diameter of approximately 12 μm and a waist length of approximately 5 mm. The tapered fiber is then fixed to an aluminum plate to be embedded in the ZnO/PDMS mixture using the drop-casting technique. To maximize the coated surface area, the tapered fiber with the adhered ZnO/PDMS mixture is rolled gently and moved laterally from end to end against the aluminum plate, and this is repeated several times. This all surface technique enables a large interaction area between the evanescent field wave and the ZnO-SA, which in turn would enhance the nonlinearity of the device. The coated tapered fiber is then left to dry at room temperature for 3 days without requiring further heat treatment process to let the excess $CHCl_3$ fully evaporates as well as to solidify the ZnO/PDMS polymer-composite around the tapered fiber.

3. Nonlinear saturable absorption and structural characterization of ZnO/PDMS-clad tapered fiber

The saturable absorption properties of our SA device are experimentally characterized using a power-dependent transmission system based on an equalized dual-detector technique.

This technique employs a home-made mode-locked pulse system comprising of an EDFL with an integrated carbon nanotube (CNT)-based SA as the pulse source. The mode-locked pulse operates at a pulse repetition rate of 13.3 MHz and pulse duration of 594 fs. This ultrafast laser source is used to generate a signal up to 150 mW to fully saturate the ZnO-based SA. A 50:50 optical coupler and optical power meters are used to complete the measurement setup. The ZnO/PDMS-clad tapered fiber is coupled to the pulse source through one output port of the 50:50 optical coupler, and the other port is used to measure the power as a reference. By varying the input power to the SA device, the transmitted power is recorded as a function of the input power. The experimental data is shown in Fig. 1, which can be well-fitted by a solid curve based on the instantaneous two-level SA model[38] as expressed in Eq. (1) to extrapolate the approximate values of α_0, I_{sat} and α_{ns},

$$\alpha(I) = \frac{\alpha_0}{1 + \dfrac{I}{I_{\text{sat}}}} + \alpha_{\text{ns}}, \tag{1}$$

where $\alpha(I)$ is the intensity-dependent absorption coefficient, α_0 is the modulation depth, I_{sat} is the saturation intensity, and α_{ns} is the non-saturable absorption loss. From the fitting, the modulation depth, saturation intensity, and non-saturable absorption loss of the device are estimated to be 6.4%, 4.15 MW/cm^2, and 55.48%. This indicates a strong saturable absorption property of the device, which can be potentially used for short-pulse laser generation. The obtained modulation depth is comparable to the widely used graphene and CNT-based SA as reported in Refs. [34,39,40]. It is expected that higher modulation depth can be achieved by increasing the concentration of ZnO, though this comes at the expense of increasing its insertion loss. The measured insertion loss of our SA device is about $\sim$ 0.87 dB.

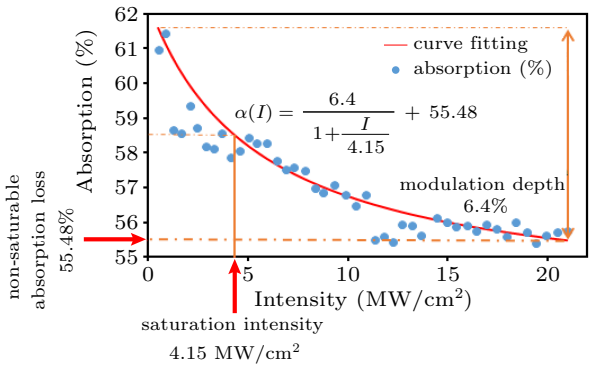


Fig. 1. Nonlinear saturable absorption characterization of ZnO/PDMS-clad tapered fiber SA.

The prepared SA device is further examined microscopically under Raman spectroscopy by a Witec Alpha 300R Raman spectrometer. The Raman spectrum is acquired by a laser excitation at 531.88 nm with an exposure time of 5.1 s using a grating value of 600 g/mm, and the incident power and the depth of field are set to be 1 mW and 16.25 μm, respectively. Figure 2 shows the Raman spectrum of the prepared SA device, which exhibits several significant intensity peaks at Raman shift of approximately 100, 191, 491, 2905, and 2966 cm^{-1}. The vibrational modes at 100 cm^{-1} and 491 cm^{-1} are found to match the specified Raman peak profile for ZnO, with each associated with the vibration of the heavy Zn sublattice at E_2 (low) and oxygen atoms at E_2 (high) respectively,[41,42] thus confirming the presence of ZnO on the tapered fiber. It is remarkable that the blue-shift in E_2 (high) from 437 cm^{-1} (theoretical value) to 491 cm^{-1} (experimental value) is created by the impurities or the tensile strain in the sample.[43] On the other hand, the observed intensity peaks at 2905 cm^{-1} and 2966 cm^{-1} are assigned to the C–H vibration of the Vinyl group in the PDMS.[44] In addition, Raman spectroscopy can also be used to characterize the disorder and defects of the ZnO samples.

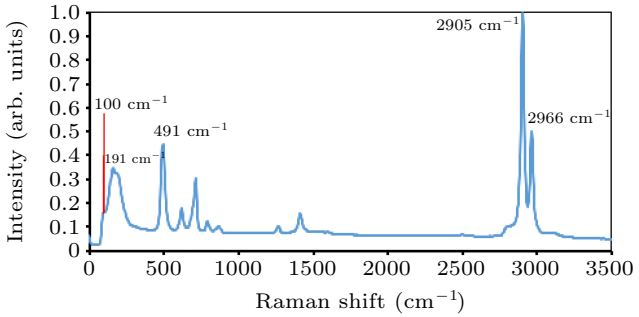


Fig. 2. Raman trace of ZnO/PDMS-clad tapered fiber.

Figure 3(a) presents the surface of ZnO/PDMS-clad tapered fiber measured by the field emission scanning electron microscope (FESEM) at a scale bar of 40 μm. It can be observed that the coated ZnO/PDMS reveals a smooth surface and a uniform structure appearance along the tapered region. For comparison purposes, the FESEM image of a bare tapered fiber is shown in Fig. 3(b).

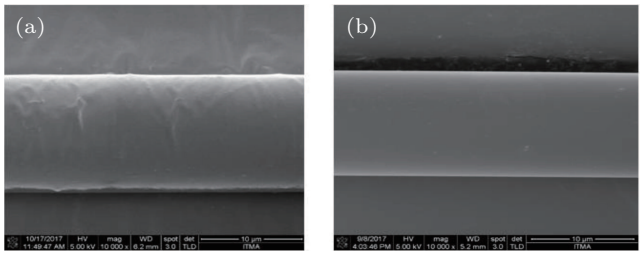


Fig. 3. Top view FESEM image of (a) ZnO/PDMS-clad tapered fiber and (b) bare tapered fiber.

4. Experimental setup

Figure 4 illustrates the experimental setup of the mode-locked EDFL based on ZnO/PDMS-clad microfiber as the SA. A section of 6.5 m Lucent Technologies HP980 erbium-doped

fiber (EDF) is pumped by a 980 nm laser diode (LD) through a 980 nm port of a fused 980/1550 nm wavelength division multiplexer (WDM). The signal absorption coefficient of the EDF is about 3.5 dB/m at 1530 nm. An optical isolator is spliced at the output port of the EDF to ensure unidirectional signal oscillation in the clockwise direction within the ring-structured EDFL cavity. The fabricated ZnO/PDMS-clad microfiber is placed after the isolator, whereby this ZnO-based SA assembly acts as the modelocking element in the laser cavity. After passing through the ZnO-based SA, the signal is then channeled to an 80:20 coupler for tapping out a 20% portion of the signal oscillating in the cavity for further analysis. On the other hand, the remaining signal will propagate through the 80% port of the coupler, which is connected to a polarization controller (PC). This PC functions to adjust the birefringence effect in the laser cavity as well as to optimize the mode-locking state. The signal is finally channeled back to the 1550 nm port of the WDM, thus completing the laser resonator. The length of the resonator is approximately 22.4 m.

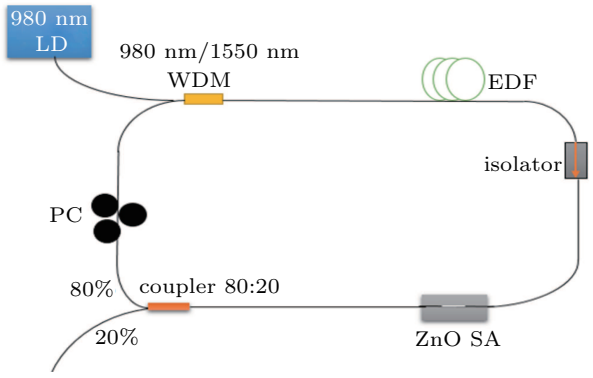


Fig. 4. Experimental setup of mode-locked EDFL using the fabricated ZnO/PDMS-clad microfiber-based SA.

A Yokogawa AQ6370B optical spectrum analyzer (OSA) with a resolution of 0.02 nm is used to measure the output spectrum of the generated mode-locked laser. Analyzing the pulse train properties of the modelocked pulses makes use of a Tektrunin TDS 3012C digital phosphor oscilloscope together with a Thorlabs SIR5 1856 light wave detector for optical to electrical conversion in place of the OSA. A GW INstek GSP-830 radio frequency spectrum analyzer (RFSA) is used to analyze the pulse train in the frequency domain. An autocorrelator (Alnair HAC-200) is also used to analyze the autocorrelation trace of the output pulse.

5. Mode-locked EDFL performance with ZnO/PDMS-clad microfiber-based SA

The proposed system initially operates in the continuous wave (CW) mode at a lasing threshold of 24.5 mW. Further increase of the pump power to 33.07 mW and above yields a mode-locking operation with an appropriate setting of the PC. At the maximum pump power of 151.5 mW, the central wavelength and 3-dB spectral width of the mode-locked spectrum are 1558.48 nm and 5.02 nm, respectively. The output spectrum of the mode-locked EDFL obtained from the OSA at the maximum pump power of 151.5 mW is shown in Fig. 5. Considering the dispersion coefficient β_2 of the EDF, SMF-28, and Hi-1060 SMF used in the laser cavity with the value of 23 ps^2/km, -22 ps^2/km, and -7 ps^2/km, respectively, the estimated total group velocity dispersion (GVD) for the entire cavity is -0.186 ps^2, thereby putting the operation of the laser in the anomalous dispersion regime and allowing the laser to operate in a soliton mode-locking regime. The Kelly sidebands observed from the optical spectrum in Fig. 5 further validate the solitonic behavior of the pulsed laser.

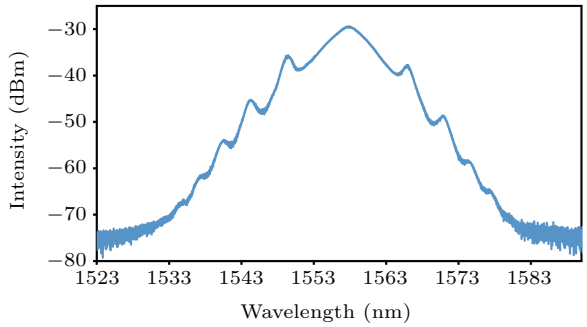


Fig. 5. Optical spectrum of the mode-locked EDFL.

The pulse time characteristic of the output solitons as measured from the autocorrelator is shown in Fig. 6, which represents the autocorrelation trace using sech^2 fitting. By assuming the sech^2 pulse shape, the full-width half maximum (FWHM) pulse duration is estimated to be 1.03 ps, which is slightly shorter than the reported value of 1.21 ps in Ref. [27]. The autocorrelation trace shows that the experimentally obtained value agrees well with the theoretical sech^2 fitting, with no indication of pulse breaking or pulse pair generation. A time-bandwidth product (TBP) of 0.63 is obtained, which indicates a minor deviation from the expected transform-limited sech^2 pulse of 0.315, due to the slight chirping in the pulse. Theoretically, the pulse chirping can be reduced by compensating the dispersion at the laser output.

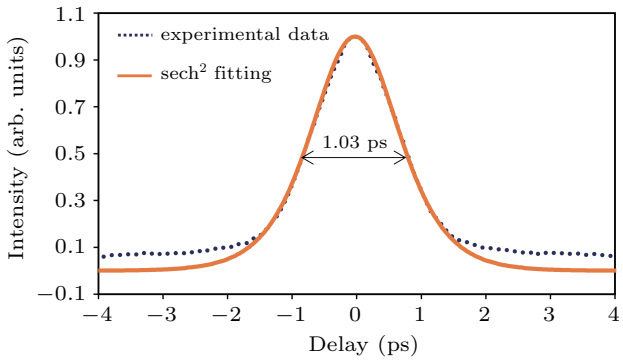


Fig. 6. Autocorrelation trace of the mode-locked pulse.

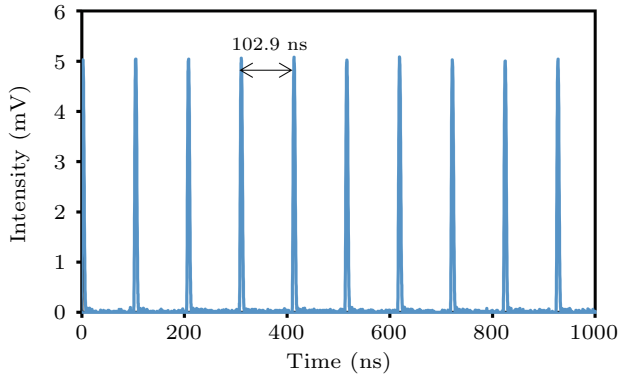


Fig. 7. Output pulse train of the mode-locked EDFL.

Figure 7 shows the output pulse train of the mode-locked EDFL obtained at the pump power of 151.5 mW. The time interval between two consecutive pulses in the pulse train is 102.9 ns, which corresponds to a pulse repetition rate of 9.77 MHz, thus matching well with the computed repetition rate for a cavity length of 22.4 m. The intensity of the peaks is almost constant at 5 mV, without any distinct amplitude fluctuation, indicating that the mode-locking operation is stable. Measurement of the average output power and pulse energy of the pulse yields a value of approximately 1.3 mW and 0.13 nJ, respectively.

The mode-locked output intensity is also measured in the frequency domain by the RFSA to further characterize the operating stability of the mode-locked pulses. Figure 8 shows the output pulse measured by the RFSA with the RF spectrum span of 50 MHz. The RF spectrum provides an evenly spaced frequency interval of approximately 10 MHz, which is comparable to the measurement of pulse repetition rate value obtained from the oscilloscope, thus indicating that the mode-locked laser output works in its fundamental regime. No spectral modulation is observed from the RF spectrum, which proves that there is no Q-switching instability in the mode-locked pulses.[45]

Figure 9 plots the fundamental cavity round-trip frequency observed at $\sim$ 10 MHz in the RF spectrum, which is measured with about 300 kHz frequency span and 0.01 kHz resolution. The peak-to-pedestal extinction ratio of the fundamental pulse is estimated to be approximately 58 dB, implying low amplitude noise fluctuations as well as low timing jitter.[46,47] It can also be seen that the RF spectrum exhibits no sidebands, signifying good stability of the pulse train.[48]

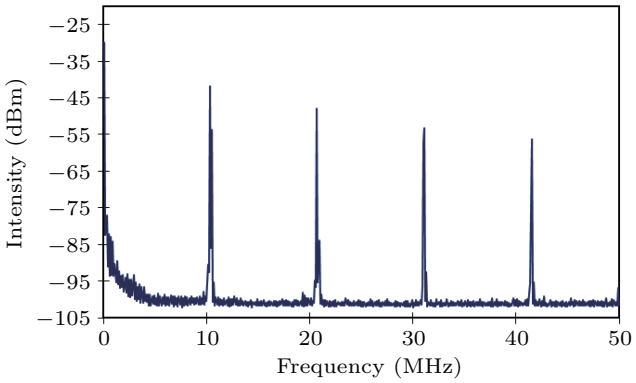


Fig. 8. RF spectrum of the mode-locked pulses at 50 MHz span.

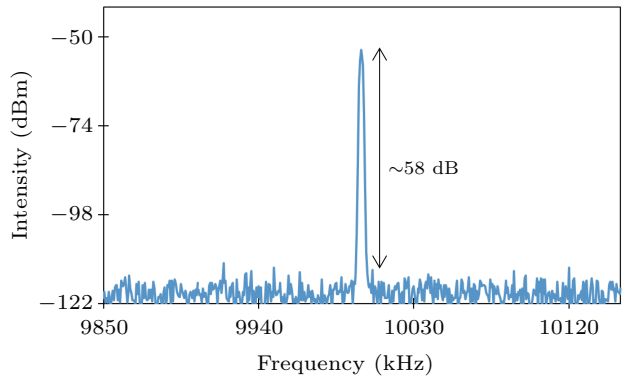


Fig. 9. RF spectrum at fundamental frequency peak of $\sim$ 10 MHz.

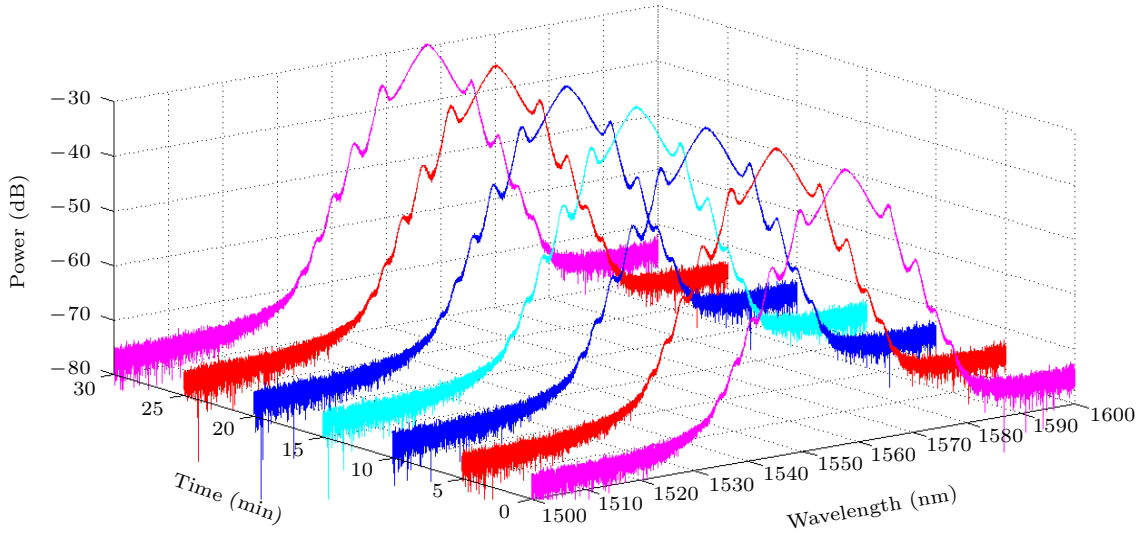


Fig. 10. Short-term stability measurement of the output spectrum over 30 minutes.

To further verify the stability of the proposed system, a short-term stability measurement of the optical spectrum is carried out at the maximum pump power of 151.5 mW within an observation period of 30 minutes for every 5 minutes time interval, and the result is shown in Fig. 10. Based on the result in Fig. 10, it can be seen that the optical spectrum behavior is well maintained over time with no obvious deviation of the output power and spectral bandwidth, in addition to a negligible shift in the central wavelength of 1558.48 nm as well as the side bands, thus validating the high stability of the mode-locked laser operation. This result also proves the high power tolerance of our SA device based on its ability to operate continuously at a high pump power of 151.5 mW, with no sign of surpassing its damage threshold. It is expected that the power tolerance ability of the SA device towards the optical power-induced thermal damage could be further enhanced by optimizing the diameter of the tapered fiber and the quality of the coated SA.[33]

6. Conclusion

In summary, we demonstrate the fabrication of ZnO/PDMS polymer-composite coated around the whole surface of the tapered fiber. We achieve this by embedding a tapered fiber in ZnO/PDMS polymer-composite solution and spreading the solution evenly throughout the tapered region for whole surface deposition. Subsequently, we propose and demonstrate the use of the fabricated ZnO/PDMS-clad tapered fiber as an SA to generate mode-locked pulses in an EDFL cavity based on evanescent field interaction. The modulation depth and saturation intensity of the fabricated SA device are measured to be 6.4% and 4.15 MWcm^{-2}, respectively. The proposed laser is able to generate soliton mode-locking operation at a threshold power of 33.07 mW, with a 3 dB spectral bandwidth of 5.02 nm and a central wavelength of 1558 nm. The generated output pulse yields a repetition rate and pulse width of 9.77 MHz and 1.03 ps, respectively. These results indicate that the proposed ZnO/PDMS-clad tapered fiber could be a useful SA device for ultrafast laser applications.

References

[1] Luo Z Q, Wang J Z, Zhou M, Xu H Y, Cai Z P and Ye C C 2012 *Laser Phys. Lett.* **9** 229
[2] Keller U 2003 *Nature* **424** 831
[3] Brida D, Krauss G, Sell A and Leitenstorfer A 2014 *Laser Photon. Rev.* **8** 409
[4] Zeng C, Liu X and Yun L 2013 *Opt. Express* **21** 18937
[5] Grelu P and Akhmediev N 2012 *Nat. Photon.* **6** 84
[6] Liu X, Cui Y, Han D, Yao X and Sun Z 2015 *Sci. Rep.* **5** 9101
[7] Okhotnikov O, Grudinin A and Pessa M 2004 *New J. Phys.* **6** 177
[8] Afifi G, AttaKhedr M, Badr Y, Danailov M, Sigalotti P, Cinquegrana P, Alsous M B and Galaly A R 2016 *Optical Fiber Technology* **29** 74
[9] Set S Y, Yaguchi H, Tanaka Y and Jablonski M 2004 *J. Lightwave Technol.* **22** 51
[10] Hasan T, Sun Z, Wang F, Bonaccorso F, Tan P H, Rozhin A G and Ferrari A C 2009 *Adv. Mater.* **21** 3874
[11] Zhang H, Bao Q, Tang D, Zhao L and Loh K 2009 *Appl. Phys. Lett.* **95** 141103
[12] Sun Z, Hasan T, Torrisi F, Popa D, Privitera G, Wang F, Bonaccorso F, Basko D M and Ferrari A C 2010 *ACS Nano* **4** 803
[13] Cui Y and Liu X 2013 *Opt. Express* **21** 18969
[14] Zhang H, Liu C, Qi X, Dai X, Fang Z and Zhang S 2009 *Nat. Phys.* **5** 438
[15] Matte H S S R, Gomathi A, Manna A K, Late D J, Datta R, Pati S K and Rao C N R 2010 *Angewandte Chemie* **49** 4059
[16] Ahmad H, Lee C S J, Ismail M A, Ali Z A, Reduan S A, Ruslan N E, Ismail M F and Harun S W 2016 *Opt. Commun.* **381** 72
[17] Johnson J C, Knutsen K P, Yan H, Law M, Zhang Y, Yang P and Saykally R J 2004 *Nano Lett.* **4** 197
[18] Wang Z L 2014 *J. Phys.: Condens. Matter* **16** 25
[19] Ahmad H, Salim M A M, Ismail M F and Harun S W 2016 *Laser Phys.* **26** 115107
[20] Aziz N A, Latiff A A, Lokman M Q, Hanafi E and Harun S W 2017 *Chin. Phys. Lett.* **34** 044202
[21] Ahmad H, Lee C S J, Ismail M A, Ali Z A, Reduan S A, Ruslan N E and S W Harun S W 2016 *Appl. Opt.* **55** 4277
[22] Song Y W, Jang S Y, Han W S and Bae M K 2010 *Appl. Phys. Lett.* **96** 051122
[23] Mao D, Wang Y, Ma C, Han L, Jiang B, Gan X, Hua S, Zhang W, Mei T and Zhao J 2015 *Sci. Rep.* **5** 7965
[24] Sotor J, Sobon G, Grodecki K and Abramski K M 2014 *Appl. Phys. Lett.* **104** 251112
[25] Luo Z Q, Wang J Z, Zhou M, Xu H Y, Cai Z P and Ye C C 2012 *Laser Phys. Lett.* **9** 229
[26] Choi S Y, Jeong H, Hong B H, Rotermund F and Yeom D 2014 *Laser Phys. Lett.* **11** 015101
[27] Liu X M, Yang H R, Cui Y D, Chen G W, Yang Y, Wu X Q, Yao X K, Han D D, Han X X, Zeng C, Guo J, Li W L, Cheng G and Tong L M 2016 *Sci. Rep.* **6** 26024
[28] Martinez A, Araimi M A, Dmitriev A, Lutsyk P, Li S, Mou C, Rozhin A, Sumetsky M and Turitsyn S 2017 *APL Photon.* **2** 126103
[29] Kashiwagi K and Yamashita S 2009 *Opt. Express* **17** 18364
[30] Khazaeinezhad R, Kassani S H, Jeong H, Park K J, Kim B Y, Yeom D and Oh K 2015 *IEEE Photon. Technol. Lett.* **27** 1581
[31] Song Y, Morimune K, Set S Y and Yamashita S 2007 *Appl. Phys. Lett.* **90** 021101
[32] Guo B, Yao Y, Yan P G, Xu K, Liu J J, Wang S G and Li Y 2016 *IEEE Photon. Technol. Lett.* **28** 323
[33] Yan P, Liu A, Chen Y, Chen H, Ruan S, Guo C, Chen S, Li I L, Yang H, Hu J and Cao G 2015 *Opt. Mater. Exp.* **5** 479
[34] Kieu K and Mansuripur M 2007 *Opt. Lett.* **32** 2242
[35] Lau K Y, Ng E K, Abu Bakar M H, Abas A F, Alresheedi M T, Yusoff Z and Mahdi M A 2018 *Opt. Laser Technol.* **102** 240
[36] Ng E K, Lau K Y, Lee H K, Abu Bakar M H, Kamil Y M, Omar M F and Mahdi M A 2020 *Opt. Mater.* **100** 109619
[37] Ribut S H, Abdullah C A C, Mustafa M, Noorfazleena S and Azman A 2018 *Mater. Res. Express* **6** 025016
[38] Garmire E 2000 *IEEE J. Sel. Quantum Electron.* **6** 1094
[39] Sun Z, Popa D, Hasan T, Torrisi F, Wang F, Kelleher E J R, Travers J C, Nicolosi V and Ferrari A C 2010 *Nano Res.* **3** 653
[40] Martinez A and Yamashita S 2011 *Opt. Express* **19** 6155
[41] Khan A 2010 *J. Pak. Mater. Soc.* **4** 1
[42] Zhang R, Yin P G, Wang N and Guo L 2009 *Solid State Sci.* **11** 865
[43] Ashkenov N, Mbenkum B N, Bundesmann C, Riede V, Lorenz M, Spemann D, Kaidashev E M, Kasic A, Schubert M and Grundmann M 2003 *J. Appl. Phys.* **93** 126
[44] Cai D, Neyer A, Kuckuk R and Heise H M 2010 *J. Mol. Struct.* **976** 274
[45] Hönninger C, Paschotta R, Genoud F M, Moser M and Keller U 1999 *J. Opt. Soc. Am. B* **16** 46
[46] Sun Z, Hasan T, Wang F, Rozhin A G, White I H and Ferrari A C 2010 *Nano Res.* **3** 404
[47] von der Linde D 1986 *Appl. Phys. B* **39** 201
[48] Zhang M, Kelleher E J R, Torrisi F, Sun Z, Hasan T, Popa D, Wang F, Ferrari A C and Taylor J R 2012 *Opt. Express* **20** 25077